Journal of Geophysical Research

Supporting Information for

Spatial and Temporal Variability in Tide-induced Icequake Activity at the Astrolabe Glacier, East Antarctica

Tifenn Le Bris[1], Guilhem Barruol[1], Florent Gimbert[1], Emmanuel Le Meur[1], Dimitri Zigone[2], Anuar Togaibekov[1], Denis Lombardi[3]

1. Univ. Grenoble Alpes, CNRS, INRAE, IRD, Grenoble INP, IGE, 38000 Grenoble, France
2. Université de Strasbourg/CNRS, Institut Terre et Environnement de Strasbourg, UMR7063, 67084 Strasbourg Cedex, France
3. SEISTREAM, Versailles, France

Contents of this file

Text S1

Figures S1 to S5

Tables S1 to S2

Text S1:

We process GPS phase observables sampled at 30-second intervals in kinematic mode using the TRACK module of the GAMIT/GLOBK software, which incorporates double-differencing techniques to eliminate phase biases caused by drifts in the satellite and receiver clock oscillators (Chen, 1999; Herring et al., 2018). The position of survey sites on the glacier is determined with respect to the reference station DUMG, located about 8-10 km down-glacier on bedrock. Over this distance, ionospheric conditions can vary significantly between the two ends of the baseline; therefore, we use the ionosphere-free linear combination (LC) to mitigate differential ionospheric delay. The most conservative uncertainties associated with position estimates at each epoch are approximately ±10 mm in the horizontal direction and ±20 mm in the vertical direction. We use a Gaussian low-pass filter with a 6-hour moving kernel to attenuate high-frequency noise in kinematic position estimates while preserving short-term physical signals (Bartholomew et al., 2012; Andrews et al. 2014).

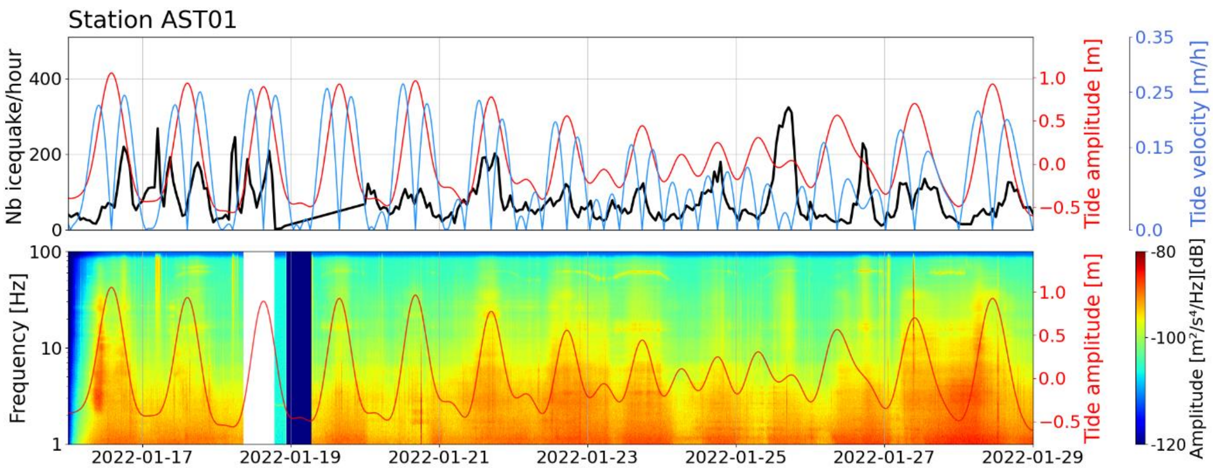

Figure S1: Tide amplitude, tide velocity, icequake rate and spectral energy at AST01 for the period January 16 to 29, 2022. Top plot: Number of detected seismic events (black curve) per hour compared with tide amplitude (red curve) and tide vertical velocity (blue curve). Bottom plot: Spectrogram of seismic energy alongside tide amplitude (red curve). Spectrogram is generated using the Logarithmic Power Spectral Density (LPSD) method on the vertical (Z) component of the data, with 10-minute windows covering the 1-100 Hz frequency range. Welch's method is applied on 10-second segments within each window, and the mean power is computed and converted to decibels (dB). The instrumental response is removed.

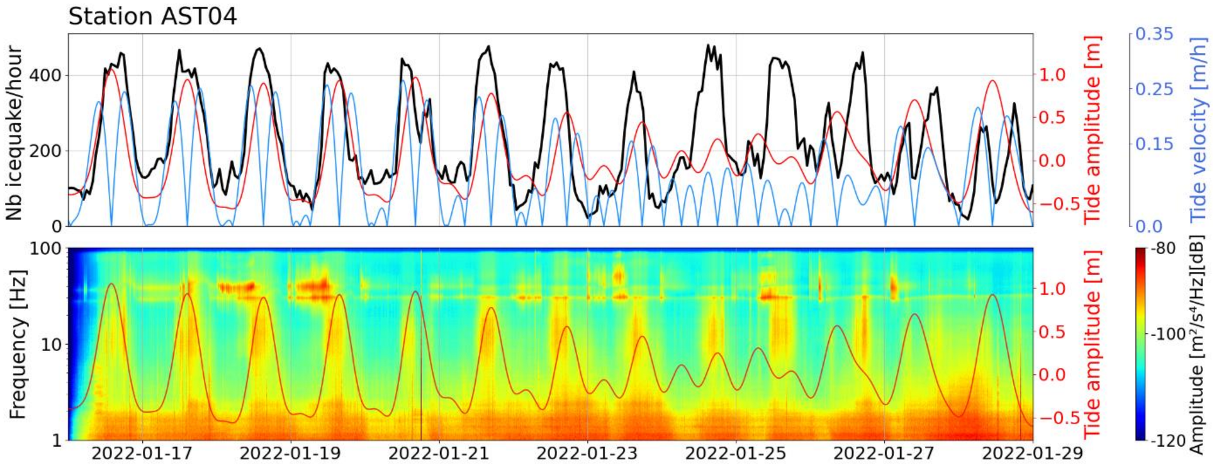

Figure S2: Tide amplitude, tide velocity, icequake rate and spectral energy at AST04 for the period January 16 to 29, 2022. Top plot: Number of detected seismic events (black curve) per hour compared with tide amplitude (red curve) and tide vertical velocity (blue curve). Bottom plot: Spectrogram of seismic energy alongside tide amplitude (red curve). Spectrogram is generated using the Logarithmic Power Spectral Density (LPSD) method on the vertical (Z) component of the data, with 10-minute windows covering the 1-100 Hz frequency range. Welch's method is applied on 10-second segments within each window, and the mean power is computed and converted to decibels (dB). The instrumental response is removed.

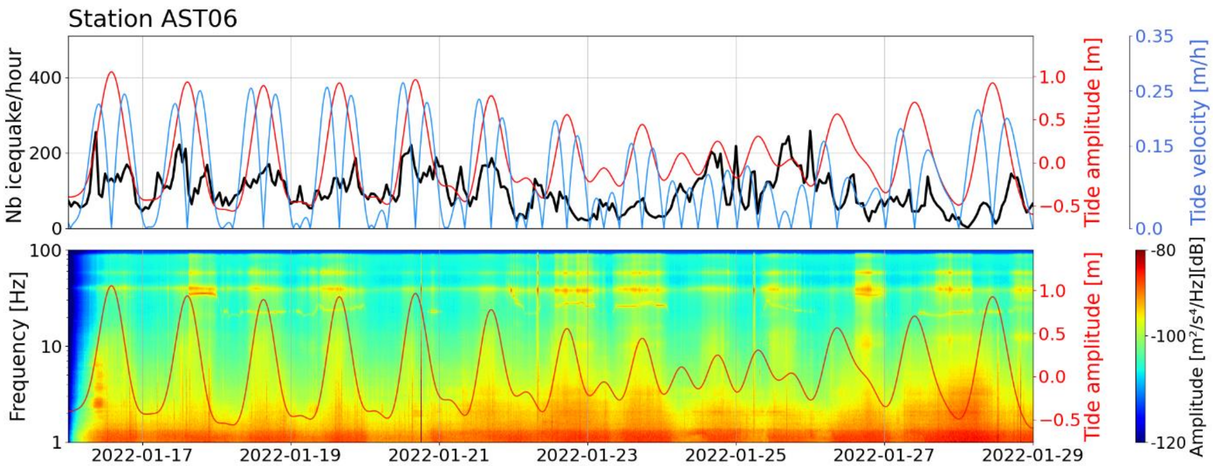

Figure S3: Tide amplitude, tide velocity, icequake rate and spectral energy at AST06 for the period January 16 to 29, 2022. Top plot: Number of detected seismic events (black curve) per hour compared with tide amplitude (red curve) and tide vertical velocity (blue curve). Bottom plot: Spectrogram of seismic energy alongside tide amplitude (red curve). Spectrogram is generated using the Logarithmic Power Spectral Density (LPSD) method on the vertical (Z) component of the data, with 10-minute windows covering the 1-100 Hz frequency range. Welch's method is applied on 10-second segments within each window, and the mean power is computed and converted to decibels (dB). The instrumental response is removed.

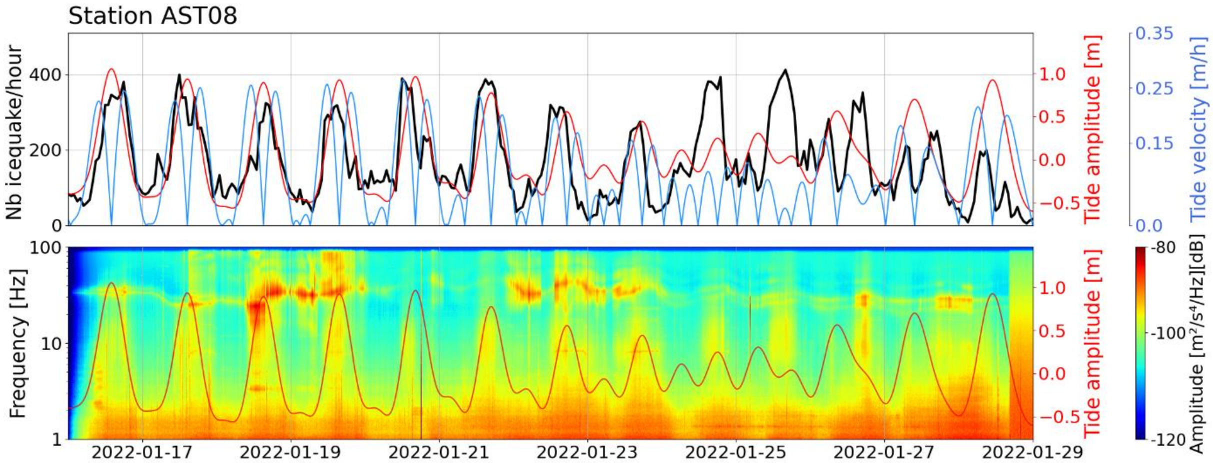

Figure S4: Tide amplitude, tide velocity, icequake rate and spectral energy at AST08 for the period January 16 to 29, 2022. Top plot: Number of detected seismic events (black curve) per hour compared with tide amplitude (red curve) and tide vertical velocity (blue curve). Bottom plot: Spectrogram of seismic energy alongside tide amplitude (red curve). Spectrogram is generated using the Logarithmic Power Spectral Density (LPSD) method on the vertical (Z) component of the data, with 10-minute windows covering the 1-100 Hz frequency range. Welch's method is applied on 10-second segments within each window, and the mean power is computed and converted to decibels (dB). The instrumental response is removed.

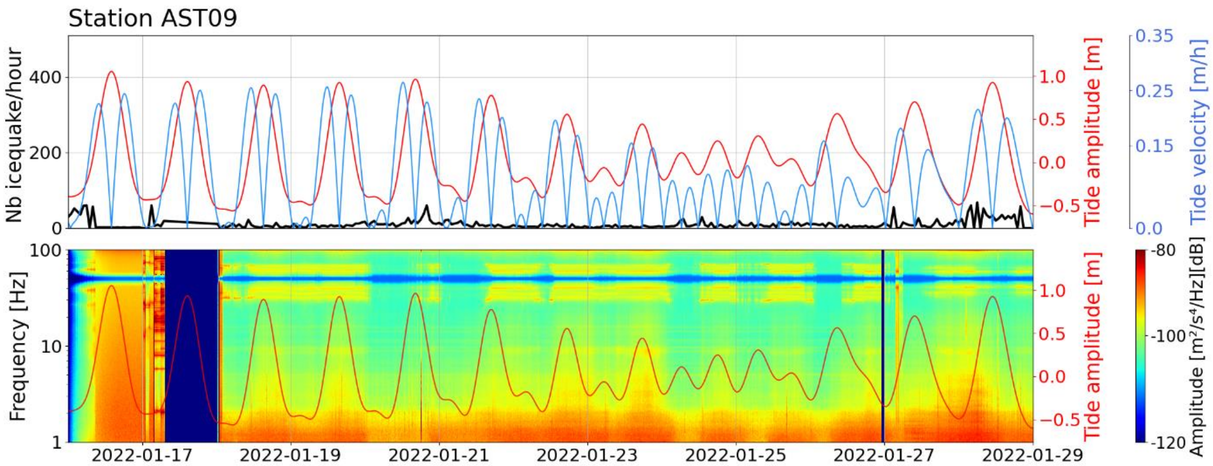

Figure S5: Tide amplitude, tide velocity, icequake rate and spectral energy at AST09 for the period January 16 to 29, 2022. Top plot: Number of detected seismic events (black curve) per hour compared with tide amplitude (red curve) and tide vertical velocity (blue curve). Bottom plot: Spectrogram of seismic energy alongside tide amplitude (red curve). Spectrogram is generated using the Logarithmic Power Spectral Density (LPSD) method on the vertical (Z) component of the data, with 10-minute windows covering the 1-100 Hz frequency range. Welch's method is applied on 10-

second segments within each window, and the mean power is computed and converted to decibels (dB). The instrumental response is removed.

Deployment	**Installation date**	**Removel date**	**Total duration**	**Type of instrument**
		Geoscope station		
G.DRV	1986	-	ongoing	Streickeisen STS1
		Broad band stations		
AST01	2020-01-18	-	ongoing	Nanometrics Trillium 120PA
AST02	2022-01-07	-	ongoing	Nanometrics Trillium Horizon 120
AST03	2022-01-12	2022-02-01	21 days	Nanometrics Trillium compact
AST04	2022-01-13	2022-02-01	20 days	Nanometrics Trillium 120QA
AST05	2022-01-11	2022-01-31	21 days -sensor tilted	Nanometrics Trillium 120QA
AST06	2022-01-13	2022-02-01	20 days	Nanometrics Trillium 120QA
AST07	2022-01-12	2022-02-01	21 days	Nanometrics Trillium 120QA

AST08	2022-01-11	2022-02-01	22 days	Nanometrics Trillium 120QA
AST09	2022-01-15	2024-01-24		Nanometrics Trillium 120PA
AST10	2022-01-15	-	ongoing	Nanometrics Trillium 120PA
AST13	2023-02-02	-	ongoing	Nanometrics Trillium 120QA
Dense Array				
Array of 50 seismic nodes	2023-01-10	2023-02-02	22 days	SmartSolo IGU-16HR-3C 5Hz
Ocean Bottom seismometers				
OBS01	2022-01-10	2022-01-29	20 days	OBS INSU
OBS02	2022-01-18	2022-01-30	13 days	OBS GURALP
OBS03	2022-01-18	2022-01-29	12 days	OBS INSU
OBS04	2022-01-10	2022-01-29	20 days	OBS INSU
OBS05	2022-02-01	2023-01-05	339 days	OBS INSU
OBS06	2022-02-01	2022-10-07	249 days	OBS GURALP

Table S1: Summary of seismic stations deployed during the SEIS-ADELICE project, including installation and removal dates, total recording days, and instrument types.

Number of Sensors Detecting an Event (Range)	Percentage of Events	Average Event Duration (s)	Average Event Duration Magnitude
[1-10]	63%	0.60	0.45
[11 – 20]	25%	0.76	0.66
[21-30]	7%	0.90	0.80
[31-40]	3%	1.08	0.96
[41-50]	2%	1.56	1.28

Table S2: Statistics for January 17, 2023. Percentage of events, average event duration and average event magnitude of duration across different bins of number of stations detecting a given event.